Bremsstrahlung in the α-α and ^{3}He-α Interactions

B. Frois,* J. Birchall,† C. R. Lamontagne, U. von Moellendorff, R. Roy, and R. J. Slobodrian
Université Laval, Département de Physique, Laboratoire de Physique Nucléaire,
Québec 10, P. Q., Canada G1K 7P4

The cross section of the bremsstrahlung process ^{4}He$(\alpha, \alpha\alpha)\gamma$ has been measured at five energies between 11.4 and 13.5 MeV with detector lab angles of $\theta_1 = \theta_2 = 37°$, and at 9.35 MeV with $\theta_1 = \theta_2 = 35°$. The results agree well with predictions based on the work of Feshbach and Yennie, Signell, and Green. No significant enhancement is found at the final state energy corresponding to the 2.9 MeV resonance in ^{8}Be. A single measurement of the process ^{4}He$(\tau, \alpha\alpha)\gamma$ made at 7.4 MeV with $\theta_1 = \theta_2 = 37°$ is also in good agreement with theory. Details of the experimental technique and of finite geometry corrections are discussed.

$$\begin{bmatrix} \text{NUCLEAR REACTIONS } ^3\text{He-}\alpha \text{ and } \alpha\text{-}\alpha \text{ bremsstrahlung, } E = 7.4, \ 9.35, \ 11.4\text{--}13.5 \\ \text{MeV, measured } d^2\sigma/d\Omega_1 d\Omega_2. \end{bmatrix}$$

1. INTRODUCTION

The study of bremsstrahlung (BS) emission in the collision of two nuclei can give information on the off-energy-shell elements of their transition matrix. These matrix elements are basic to the understanding of the interaction since they are needed in any problem involving more than these two particles.

Because of the essential role of the nucleon-nucleon interaction, the two-nucleon system was the first case investigated. But the α-α interaction, though less fundamental, also plays an important role in nuclear physics and a deeper understanding of this interaction might improve our knowledge on α clusters and possibly[1] on the interaction between complex nuclei such as ^{12}C -^{12}C or ^{16}O -^{16}O. The α-α system has a high threshold for particle emission, $E_{lab} = 34.7$ MeV. The α particle has no bound excited states and the α-α scattering amplitude is well described by broad α-particle states of ^{8}Be. This enables one to investigate the behavior of the α-α bremsstrahlung cross section in a wide energy interval where: (i) bremsstrahlung emission is the only reaction channel open; (ii) the internal structure of the α particle can be neglected which leads to important theoretical simplifications; (iii) one can find experimental situations where the initial state or the final state, or both are resonant. It has been suggested by Green[2] that the bremsstrahlung amplitude might be enhanced in these situations and it might be possible to find important model-dependent effects due to internal emission.

Experimental data of the α-α bremsstrahlung cross-section are scarce,[3-6] but measurements performed by Peyer et al.[5] between 12 and 19 MeV for final-state energies sweeping across the 2^+ first excited state of ^{8}Be, show a strong enhancement of the cross section.

In this work, we have undertaken the measurement of the α-α bremsstrahlung cross section at various energies between 9.35 and 13.5 MeV by detecting the two final-state charged particles.[7] The angles of detection were chosen so that at 12 MeV the final state was centered on the first excited state of ^{8}Be.

We report here also a measurement of the ^{3}He-α bremsstrahlung cross section at $E_{^3\text{He}} = 7.4$ MeV with counters at $\theta_1 = \theta_2 = 37°$.

2. EXPERIMENTAL PROCEDURE

A doubly ionized helium beam was provided by the CN van de Graaff of Université Laval equipped with an upgraded tube. After momentum analysis through a 90° magnet, the beam passed through a deflecting magnet and was then focused by a quadrupole lens through two pairs of slits S_1, S_2 (Fig. 1) defining a fixed direction. The beam current on the slits was constantly monitored in order to verify that the beam remained centered. The intensity of the beam was about 300 nA. The 50-cm-diam scattering chamber was filled with helium gas. To avoid build up of contaminants, fresh gas was flown through the chamber continuously, with a Cartesian manostat[8] maintaining a pressure of 100 Torr. Two windows of Havar[9] alloy foil 2.5 μm thick isolated the gas from the vacuum of the accelerator and of the Faraday cup. The beam spot was typically 1.2 mm × 1.2 mm on the foil at the entrance of the chamber situated at

31.4 mm from the center C of rotation of the de-
tectors. Two silicon surface-barrier counters
detected the two final-state charged particles at
equal polar angles on opposite sides of the beam
axis. Each detector viewed the target region
through a collimator consisting of a 4.7-mm-wide
vertical front slit FS, one antiscattering aperture
AS, and a 7-mm-diam circular rear aperture BS.
The rear aperture was 90 mm from the target
center C. The distance between front and rear
aperture was 60 mm. A detected event consisted
of three quantities measured in coincidence: the
energies E_1, E_2 of final-state charged particles,
and the time difference T between the detector
signals.

In such experiments, the accumulation rate is
very low, a few events per hour, the energies of
the particles are small (3–5 MeV), and the number
of elastic events is enormous compared with the
number of bremsstrahlung events. Some of the
elastically scattered particles have their energy
degraded by multiple scattering, slit-edge pene-
tration, reactions in the detectors, etc. This
implies the following difficulties.

(i) The energy thresholds of the fast-timing
discriminators must be kept as low as possible
in order to be sure that no BS event will be re-
jected. Such thresholds admit part of the noise
pulses. The background resulting from this was
significantly reduced by the use of additional "slow"
timing from the linear energy signals after the
amplifiers and a coincidence between the "fast"
and "slow" timing.

(ii) Very low-energy charged particles in large
number affect the timing resolution, independently
of the discriminator threshold. This was proven
by degrading the energy of an intense group of
elastically scattered particles to the point of
entering the detector with only a small residual
range. A significant improvement was accom-
plished by the addition of a very thin Ni foil (1 μm)
in front of the silicon detectors so as to stop these
particles before they reached the detectors.

(iii) Accidental coincidences between two energy-
degraded elastic events populate the E_1, E_2 plane
and thus degrade the real to background ratio for
the kinematically allowed region. These coinci-
dences increase like the square of the beam in-
tensity. This demands the best resolution possible
in the time spectrum in order to be able to use
reasonable beam intensities. The use of Ortec 130
detector systems with ARC timing[10] and a com-
puter time-of-flight correction enabled us to use
time windows less than 2 ns wide; this is an im-
provement of a factor of 3 over our previous ex-
periments.[3,4]
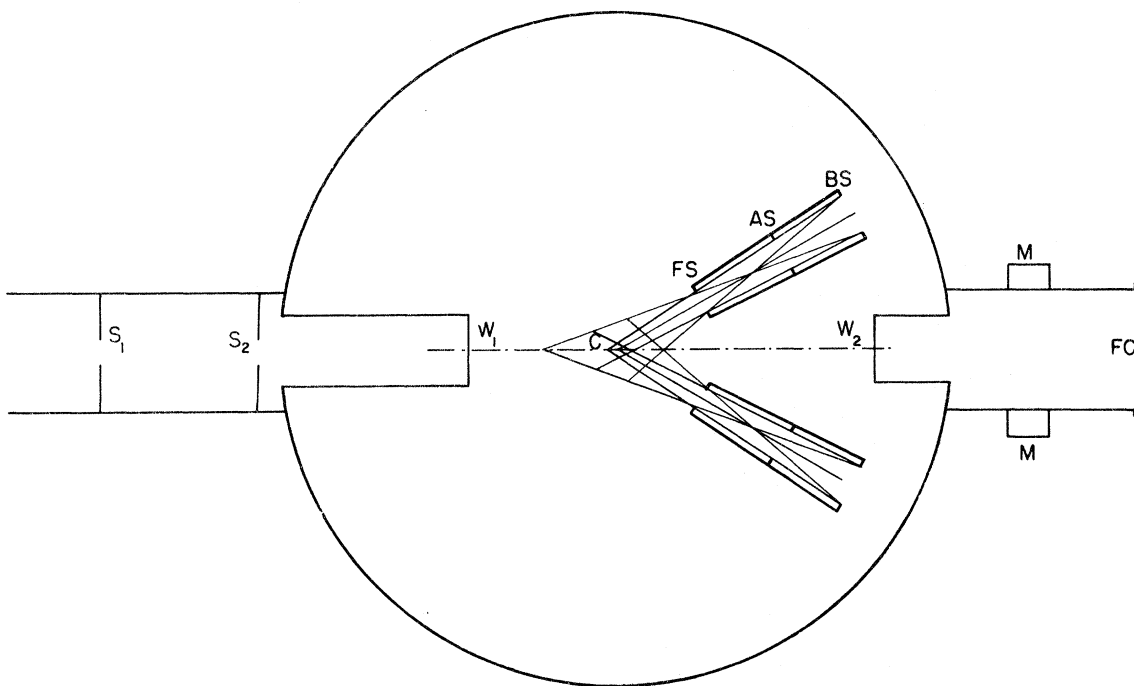
FIG. 1. Schematic view of the scattering chamber and of the collimators. S_1, S_2: defining slits; W_1, W_2: Havar
windows; C: center of rotation of the detectors; FS: vertical front slit; AS: antiscattering aperture; BS: circular
back aperture; FC: Faraday cup; M: secondary-electron-trapping magnet.
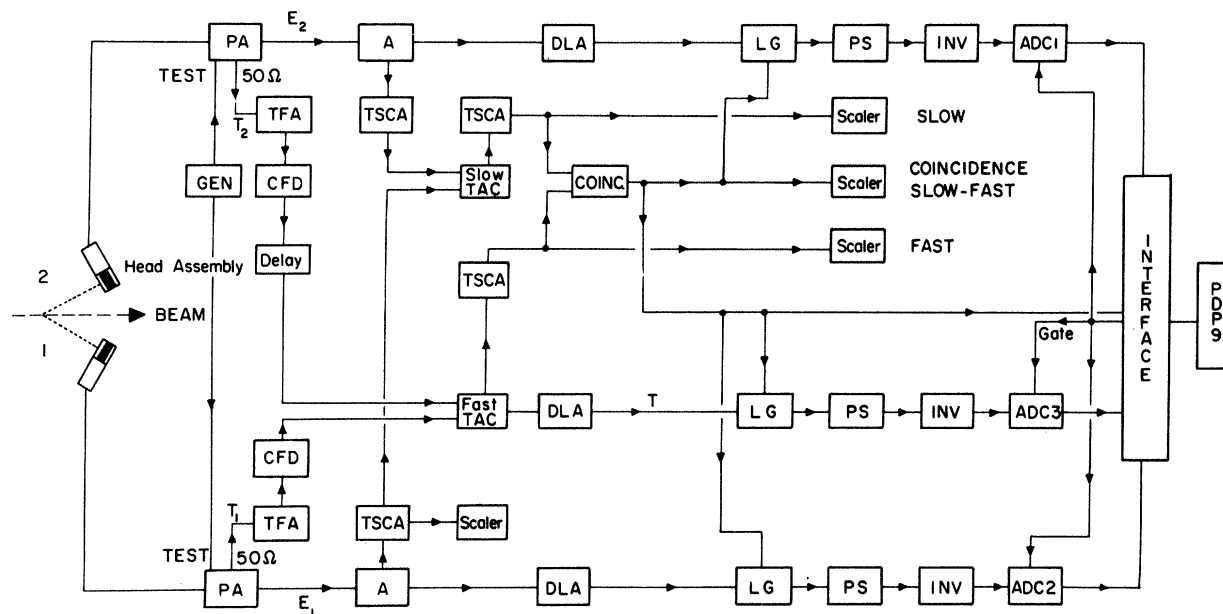
FIG. 2. Block-diagram of the electronics. GEN: pulse generator; PA: preamplifier; TFA: timing filter amplifier; CFD: constant fraction timing discriminator; A: amplifier; TSCA: timing single channel analyzer; TAC: time-to-amplitude converter; COINC: coincidence unit; DLA: delay line amplifier; LG: linear gate; PS: pulse stretcher; INV: inverter; ADC: analog-to-digital converter.

A block diagram of the detectors and electronics is shown in Fig. 2. Detectors were 270 μm thick. The electronic circuitry used to record the data was described in Refs. 3, 4, and 7. This system consists essentially of standard Ortec equipment and it utilizes fast timing derived from the two 130 systems, parallel "slow" timing from the linear energy signals, coincidence between the fast and slow timing to provide energy selection and rejection of noise pulses from the fast discriminations, three analog-to-digital converters (ADC's), and a PDP-9 computer to record and store the events. A time spectrum of 100 ns was recorded.

The peaks of α-α elastic scattering at various incident energies between 6 and 13.5 MeV were used to calibrate both the time and energy spectra. Detectors 1 and 2 were positioned at different sets of complementary angles to detect the scattered and recoil particles in coincidence. The position of the peak in the time spectrum was investigated as a function of the energies E_1 and E_2. Figure 3 illustrates the shift of the peak as a function of the calculated difference of time of flight of the two particles. Agreement is better than 200 ps which shows that walk effects were negligible and that the shift is purely due to the time-of-flight difference.

For each run a further test was made with a

continuous range of α energies from 1 to 5 MeV using the tails of the elastic peaks[11] selected by the timing single channel analyzer (TSCA's) and
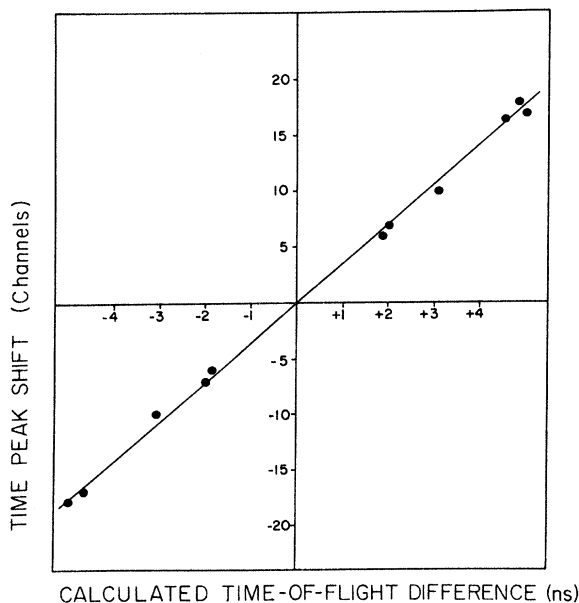
FIG. 3. Measured shift of the time peak, plotted against the calculated time-of-flight difference of the detected particles.

measured at 45–45° in coincidence. The count rate was high enough to neglect effects of the noise pulses not rejected by the constant-fraction discriminators. Two separate measurements were made, one with a gating by the "slow" time-to-amplitude converter (TAC) only, and another one by the logic pulse from the "slow" and "fast" TAC coincidence. The two-dimensional E_1-E_2 plots obtained for each run were compared. The numbers of events in the bremsstrahlung kinematically allowed region were statistically identical for the two measurements. This proved that no interesting event would be rejected by the coincidence requirement between the two TACs.

For each incident energy, the α-α elastic scattering cross section at 90° c.m. was measured to check the absolute calibration. Single spectra at 45° were recorded simultaneously by both detectors, to average over geometry effects. The cross sections were deduced from Silverstein's[12] calculations of the gaseous geometry factor using finite-beam corrections. The agreement with previous measurements[13] was always within 5%.

3. RESULTS AND DISCUSSION

A. α-α System

Six measurements of the α-α bremsstrahlung cross section were made, one at 9.35 MeV and $\theta_1 = \theta_2 = 35°$, the others at $\theta_1 = \theta_2 = 37°$ for energies between 11.44 and 13.5 MeV. Each measurement was divided into several runs that were analyzed separately in order to check consistency. In two cases, runs were separated in time by several months and results were statistically compatible.

The data were analyzed off-line with a PDP-15 computer which shares the peripheral units with the PDP-9. The analysis began by correcting the time-of-flight difference and converting the E_1 and E_2 channel numbers to energies, then building the time spectrum from all events inside the kinematically allowed region. Finally a time window centered on the coincidence peak was selected so as to give the optimum real-to-random ratio.

Figure 4 shows the two-dimensional display of results from one of the runs at 12 MeV and $\theta_1 = \theta_2$ = 37° in the lab system. The boundary of the kinematically allowed region is indicated. The time window is 1.8 ns. For the background subtraction, however, the number of random events was determined with much better statistics by averaging over two large regions (40 ns each), one on each side of the time peak. This was possible because the time spectrum outside the peak did not show any structure.

The bremsstrahlung cross section has been calculated from the yield of events through the rela-
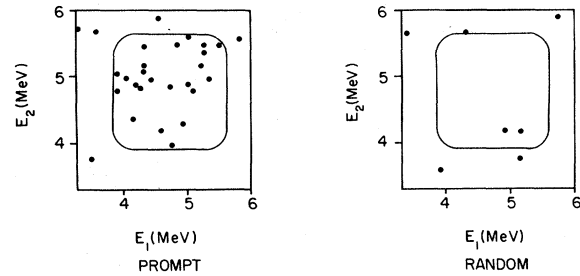
FIG. 4. Two-dimensional plot of α-α bremsstrahlung events of a typical run at 12 MeV. The energy scales are reduced to the center of the target. The boundary of the kinematically allowed region is represented by a solid line. The prompt region corresponds to a 1.8-ns time interval. The random region is a time interval of the same width delayed in the time spectrum. The method of background subtraction is discussed in the text.

tion:

$$\frac{d^2\sigma}{d\Omega_1 d\Omega_2} = \frac{Y}{nNF} \, ,$$

where n is the number of target nuclei per unit volume, N is the number of particles in the beam, and F has the dimension of a length and is a factor containing details of the two-counter geometry.[14]

$$F = \iiint \Lambda(\phi, \theta_0, \theta_1, \theta_2) d\Omega_1 d\Omega_2 dz \, ,$$

where it is assumed that the bremsstrahlung cross section can be written as:

$$\frac{d^2\sigma}{d\Omega_1 d\Omega_2} = \sigma_0(\theta_0)\Lambda(\phi, \theta_0, \theta_1, \theta_2) \, ,$$

where ϕ is the noncoplanarity angle as defined in Ref. 15; dz is a line element along the beam path; $\sigma_0(\theta_0)$ is the coplanar bremsstrahlung cross section for an angle of detection θ_0 for both detectors. $\Lambda(\phi, \theta_0, \theta_1, \theta_2)$ describes the variation of the bremsstrahlung cross section with the non-coplanarity angle and with the polar angle of each detected particle for both counters set to the nominal angle θ_0.

The uncorrected result is obtained by setting

$$\Lambda(\phi, \theta_0, \theta_1, \theta_2) = 1 \, .$$

It is not possible to compare this result to a theory since $\Lambda(\phi, \theta_0, \theta_1, \theta_2)$ equals unity only for coplanar events ($\phi = 0$) with $\theta_1 = \theta_2 = \theta_0$, whereas the finite size of the detectors and collimators allows detection of noncoplanar as well as coplanar events.

The noncoplanarity factor $f(\theta, \phi)$ defined by Green[16] has been used in the correction of the results. For quadrupole radiation, to first order in the photon energy expansion of Feshbach and
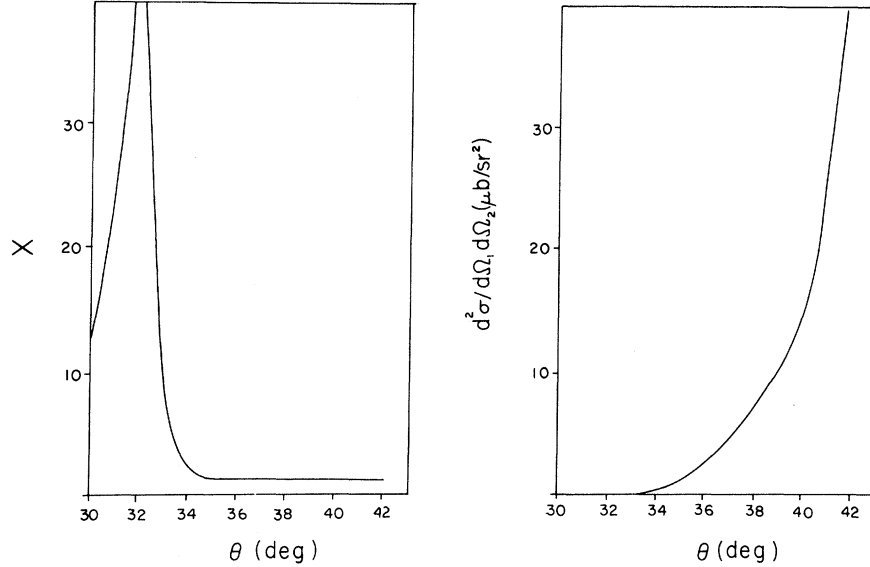
FIG. 5. $X = 3 - [4(t_i t_f^\dagger + t_i^\dagger t_f)]/(|t_i \tan^2\theta + t_f|^2) \tan^2\theta$; $d^2\sigma/d\Omega_1 d\Omega_2$ is the coplanar α-α bremsstrahlung cross section calculated to lowest order in the photon energy with Signell's formula. Both curves are given for 11.44-MeV incident α lab energy.

Yennie,[17] one has:

$$f(\theta, \phi) = [1 - (\phi/\phi_m)^2][1 + X(\theta)(\phi/\phi_m)^2] \quad \text{for } 0 < \phi \leq \phi_m,$$
(1)

and

$$f(\theta, \phi) = 0 \quad \text{for } \phi > \phi_m,$$

where ϕ_m is the maximum angle of noncoplanarity.

$$X(\theta) = 3 - \frac{4(t_i t_f^\dagger + t_i^\dagger t_f)\tan^2\theta}{|t_f + t_i \tan^2\theta|^2},$$
(2)

where t_i and t_f denote the elastic α-α amplitudes at the initial- and at the final-state energy.

The coplanar cross section $\sigma_0(\theta_0)$ was calculated from a formula given by Signell[18] based on the model-independent approach of Feshbach and Yennie.[17] The on-shell transition matrix elements at the initial- and at the final-state energy were calculated with the experimental phase shifts[1] of the s, d, and g waves interpolated by a smooth curve.

Figure 5 shows the variation of X and σ_0 as a function of θ for an incident energy of 11.44 MeV. The minimum and maximum polar angles of acceptance for each of the collimators are 31.3 and 42.7°, and X and σ_0 exhibit a very strong variation over that angular range. Correlated particles, however, must be emitted from the same point of the beam. The resulting limits of θ_1 and θ_2 as a function of each other are shown by the outer boundary in Fig. 6. The detection efficiency was

obtained by assuming that

$$\Lambda(\phi, \theta_0, \theta_1, \theta_2) = \frac{f(\theta_1, \phi) + f(\theta_2, \phi)}{2}$$

$$\times \frac{\sigma_0(\theta_1) + \sigma_0(\theta_2)}{2\sigma_0(\theta_0)}.$$
(3)

Figure 6 gives the percentage contribution to the two-counter geometry factor F of each $2° \times 2°$ square in the $\theta_1 - \theta_2$ plane, calculated with the noncoplanarity factor of Eq. (1) for $E_\alpha = 11.44$ MeV. The angular interval of $37° \pm 2°$ provides 90% of the efficiency. This limits considerably the effects of the variations of $\Lambda(\phi, \theta_0, \theta_1, \theta_2)$. The region below 35°, where X and σ_0 show an important nonlinear variation, contributes less than 1% to the over-all efficiency, so that in view of the statistical uncertainty, the simple averaging in Eq. (3) is justified.

The results obtained are summarized in Table I. The errors quoted are 1 standard deviation from counting statistics.

Figure 7 is a comparison of the experimental results to theory for $\theta_1 = \theta_2 = 37°$. The curve represents the variation of σ_0 as a function of incident energy calculated as described above. The results are in good agreement with the model-independent calculation. However, they may be also consistent with a possible structure around 12 MeV, but there is not a strong enhancement as in the results of Ref. 5 at $\theta_1 = \theta_2 = 35°$.

At 35° and 9.35 MeV our calculation from the
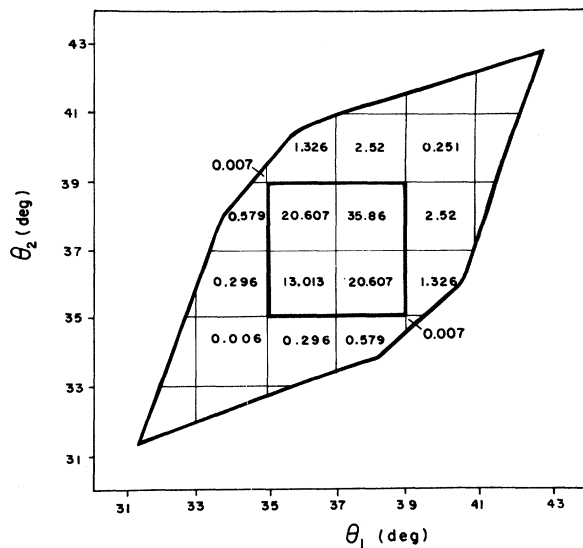
FIG. 6. Detection efficiency for α-α bremsstrahlung as a function of the angles θ_1 and θ_2 of the detected particles. The exterior solid line shows the boundary of the region accepted by the collimators of both detectors at 37°. The square defined by the heavy solid line represents 90% of the total detection efficiency. The numbers indicate the percentage of the total detection efficiency of each 2° × 2° square for a bombarding energy E_α= 11.44 MeV.

formula of Signell gives a value of 0.07 μb/sr^2 in reasonable agreement with the experimental result. But the theoretical value at that energy is very sensitive to the phase shifts used to calculate the elastic amplitudes t_i and t_f because the cross section $\sigma_0(\theta)$ is in the region of a minimum. With the same approach Green[2] has obtained a value of 0.1 and 0.085 μb/sr^2 after applying a model-dependent correction. All these values are consistent with our experimental value.
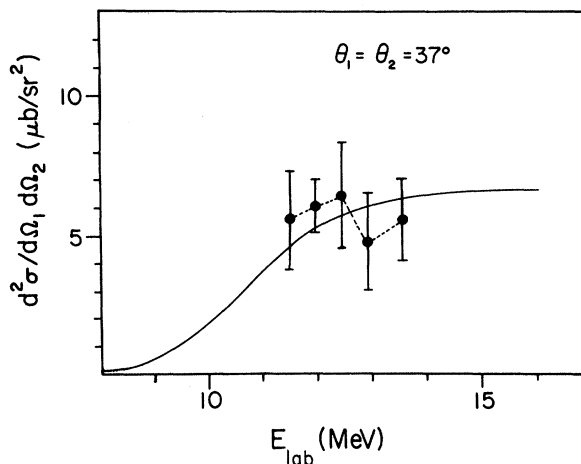
FIG. 7. Comparison of the prediction of Signell's formula for the α-α bremsstrahlung cross section at $\theta_1 = \theta_2 = 37°$ with the measured value corrected for the variation with noncoplanarity and with the polar angles of the detected particles. The dashed line has been drawn through the experimental points to guide the eye only.

B. ^{3}He-α System

The ^{3}He-α BS cross section was measured at a ^{3}He incident energy of 7.4 MeV with the counters at $\theta_1 = \theta_2 = 37°$. A preliminary result was presented previously.[19] In this system, the BS emission by a dipole transition is allowed as in the p-α and p-d systems. At our energy the initial state is just above the threshold of the reaction ^{4}He$(\tau, p)^6$Li and the final state is below the elastic resonance of the $^2f_{7/2}$ state of ^{7}Be.

Figure 8 shows the experimental result. The prompt and the random regions shown on the figure correspond to 6-ns time intervals. The

TABLE I. Measurements of cross sections of α-α bremsstrahlung. The energies quoted are at the center of the scattering chamber. The corrected cross section is obtained by taking into account the variation of the cross section with the angle of noncoplanarity and with the polar angles of the detected particles. The method of calculating this correction is described in the text. The calculated cross section is obtained from the model-independent calculation of Signell to lowest order in the photon energy.

Laboratory angles of the detectors	Bombarding α energy (MeV)	Measured cross section (μb/sr^2) Uncorrected	Corrected	Calculated cross section (μb/sr^2)
35°,35°	9.35	0.36 ± 0.23	0.17 ± 0.11	0.07
37°,37°	11.44	1.82 ± 0.59	5.6 ± 1.8	4.4
37°,37°	12.00	1.97 ± 0.32	6.2 ± 1	5.2
37°,37°	12.47	2.09 ± 0.64	6.5 ± 2	5.7
37°,37°	13.00	1.53 ± 0.59	4.7 ± 1.8	6.1
37°,37°	13.50	1.87 ± 0.52	5.4 ± 1.5	6.3
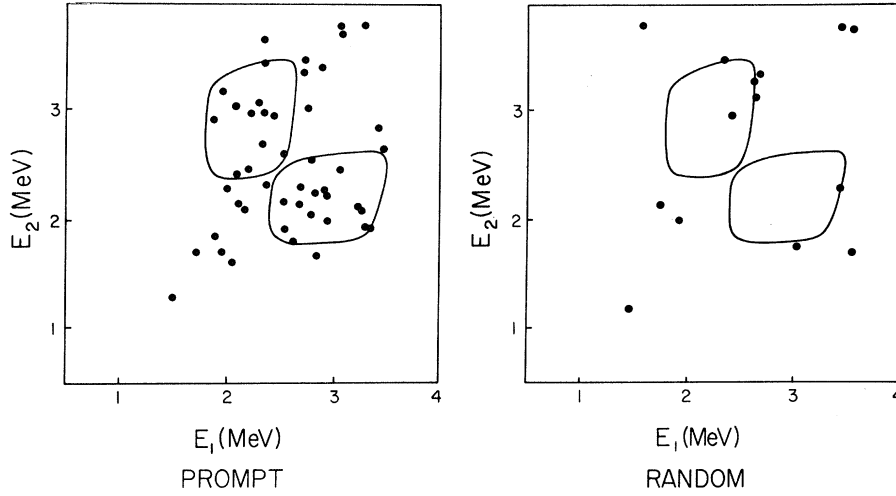
FIG. 8. Two-dimensional plot of ^{3}He-α bremsstrahlung events at 7.4 MeV. The prompt and random regions correspond to 6-ns time intervals (see Fig. 4).

evaluation of the number of true events was done as described in the previous paragraph, with an averaging of the background over 20 ns. The result was corrected with the noncoplanarity form of Green[16] for a dipole transition:

$$f(\phi) = 1 + (\phi/\phi_m)^2 \quad 0 \leqslant \phi \leqslant \phi$$

and   (4)

$$f(\phi) = 0 \quad \phi > \phi_m \; .$$

The value obtained for the coplanar cross section is 12.6 ± 3.4 $\mu b/sr^2$.

The theoretical cross section was obtained with an expression due to Green[20] for the first term of the Feshbach-Yennie[17] expansion:

$$\frac{d^2\sigma}{d\Omega_\tau d\Omega_\alpha} = \frac{1}{(2j_\tau + 1)(2j_\alpha + 1)} A \frac{P_\tau}{m_\tau} \frac{e^2}{\pi} (Z_\tau - \frac{m_\tau}{m_\alpha} Z_\alpha)^2$$

$$\times \mathrm{Tr}\{B|t_i|^2 + |t_f - Ct_i|^2\} \tag{5}$$

with

$$A = \frac{\sin^2\theta_\tau \sin^2\theta_\alpha}{\sin(\theta_\tau + \theta_\alpha)[\sin^2(\theta_\tau + \theta_\alpha) - \sin^2\theta_\alpha - (m_\tau/m_\alpha)\sin^2\theta_\tau]^2} \; ,$$

$$B = \left(\frac{m_\tau + m_\alpha}{m_\alpha}\right)^2 \frac{\sin^2\theta_\tau \sin^2\theta_\alpha}{\sin^2(\theta_\tau + \theta_\alpha)} \; ,$$

and

$$C = \frac{m_\tau + m_\alpha}{m_\alpha} \frac{\sin\theta_\alpha \cos\theta_\tau}{\sin(\theta_\tau + \theta_\alpha)} - \frac{m_\tau}{m_\alpha} \; .$$

The subscript τ indicates a ^{3}He parameter, masses are indicated by m, charges by Z, momenta by P, angular momenta by j; t_i and t_f are the elastic amplitudes. Equation 5 is written choosing $\hbar = c = 1$.

The phase shifts and inelastic parameters used to calculate the elastic amplitudes were obtained from Barnard, Jones, and Weil[21] and from Spiger and Tombrello.[22]

To be able to compare the theory with our experimental result, the theoretical cross section has been calculated for the finite geometry of the
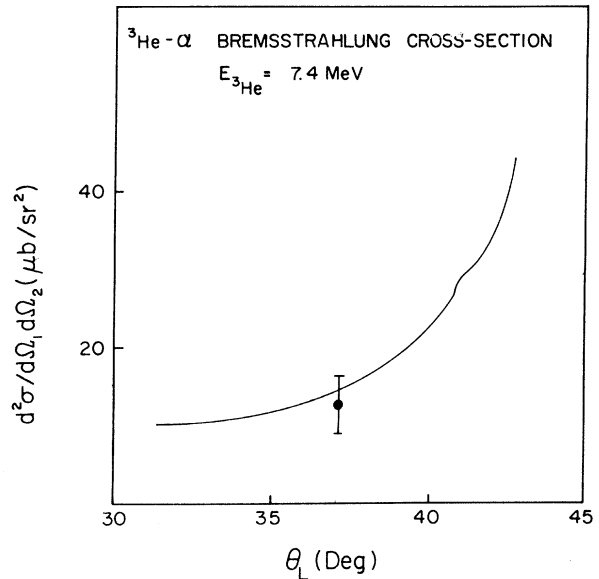
FIG. 9. Comparison of the measured ^{3}He-α bremsstrahlung cross section at 7.4 MeV, corrected only for noncoplanarity with the prediction of Green to the lowest order in the photon energy expansion. The theoretical values represented by the solid line are obtained by averaging over the kinematically allowed region as described in the text.
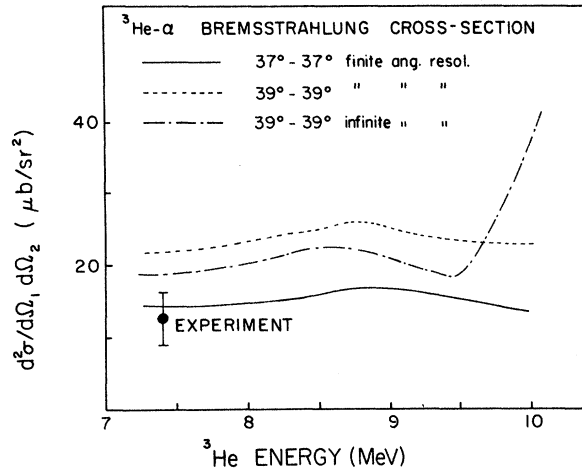
FIG. 10. See Fig. 9. The two dashed lines show the difference of the theoretical values obtained at 39°, 39° when finite geometry effects are taken into account. The sharp rise beyond 9.5 MeV (dashed-dotted line) is due to the $^2f_{7/2}$ resonance of ^{7}Be. This effect, however is smeared out by the angular acceptance of the collimators.

two counters over the kinematically allowed region. This was possible because Eq. (5) is valid for $\theta_T \neq \theta_\alpha$. The variation of the theoretical cross sec-

tion, corrected for the finite geometry as a function of the nominal angle θ of both counters is shown in Fig. 9. At 37° the theoretical value of 14.32 μb/sr^2 is slightly higher than the experimental result. This indicates that the second term of the Feshbach-Yennie expansion, which contains the rescattering term, gives a negligible contribution. The bump at 41° is due to the $^2f_{7/2}$ resonance of ^{7}Be in the final state. This effect however is experimentally very small, due to the smearing by the finite geometry.

Figure 10 shows the BS cross section as a function of energy for two pairs of detection angles, $\theta_1 = \theta_2 = 37°$ and $\theta_1 = \theta_2 = 39°$. A comparison is given at 39° with a calculation for infinite angular resolution above 10 MeV. The effect of the $^2f_{7/2}$ resonance is very strong for that case but completely damped in the case of finite geometry. The measurement of the effect of that resonance on the ^{3}He-α BS cross section would require a much better angular resolution.

*Present address: Service de Physique Nucléaire à Haute Energie, C. E. N. SACLAY, B. P. no. 2, 91190 Gif-sur-Yvette, France.

†Present address: Lawrence Berkeley Laboratory, University of California, Berkeley, California 94720.

[1]S. A. Afzal, A. A. Z. Ahmad, and S. Ali, Rev. Mod. Phys. 41, 247 (1969).

[2]A. M. Green, R. Müller, and U. Peyer, University of Helsinki, Research Institut for Theoretical Physics, Report No. 11-72 (to be published).

[3]B. Frois, J. Birchall, R. Roy, and R. J. Slobodrian, Phys. Rev. Lett. 28, 633 (1972).

[4]B. Frois, J. Birchall, R. Roy, C. R. Lamontagne, and R. J. Slobodrian, in Proceedings of the International Conference on Few Particle Problems in the Nuclear Interaction, Los Angeles, 1972, edited by I. Šlaus, S. A. Moszkowski, R. P. Haddock, and W. T. H. van Oers (North-Holland, Amsterdam, 1972).

[5]U. Peyer, J. Hall, R. Müller, M. Suter, and W. Wölfli, Phys. Lett. 41B, 151 (1972).

[6]W. Wölfli, J. Hall, R. Müller, M. Peyer, and M. Suter, in Proceedings of the International Conference on Few Particle Problems in the Nuclear Interaction, Los Angeles 1972, edited by I. Šlaus et al. (North-Holland, Amsterdam, 1972).

[7]J. Birchall, B. Frois, R. Roy, and R. J. Slobodrian, Nucl. Instrum. Methods 96, 45 (1971).

[8]Manostat Corporation, New York, N. Y.

[9]Hamilton Watch Co., Lancaster, Pa.

[10]Instruments for research, Ortec Inc., Oak Ridge, Tenn. Catalog 1002.

[11]R. J. Slobodrian, Nucl. Instrum. Methods 79, 141 (1970).

[12]E. A. Silverstein, Nucl. Instrum. Methods 4, 53 (1959).

[13]T. A. Tombrello and L. S. Senhouse, Phys. Rev. 129, 2252 (1963).

[14]J. Birchall, Nucl. Instrum. Methods 101, 493 (1972).

[15]D. Drechsel and L. C. Maximon, Ann. Phys. (N.Y.) 49, 403 (1968).

[16]A. M. Green and A. Prodon, Nucl. Phys. A183, 225 (1972).

[17]H. Feshbach and D. R. Yennie, Nucl. Phys. 37, 150 (1962).

[18]P. Signell, Advances in Nuclear Physics, edited by M. Baranger and E. Vogt (Plenum, New York, 1969), Vol. 2.

[19]J. Birchall, B. Frois, R. Roy, and R. J. Slobodrian, in Proceedings of the International Conference on Few Particle Problems in the Nuclear Interaction, Los Angeles 1972, edited by I. Šlaus et al. (North-Holland, Amsterdam, 1972).

[20]A. M. Green, Nuclear Physics Laboratory Annual Report, ETH (Zurich), 1970 (unpublished), p. 95.

[21]A. C. L. Barnard, C. M. Jones, and J. L. Weil, Nucl. Phys. 50, 629 (1964).

[22]R. J. Spiger and T. A. Tombrello, Phys. Rev. 163, 964 (1967).